F. E. Udwadia
Assist. Professor,
University of Southern California,
Los Angeles, Calif.

P. C. Shah
Graduate Student,
California Institute of Technology,
Pasadena, Calif.

Identification of Structures Through Records Obtained During Strong Earthquake Ground Motion

The problem of estimating a space dependent coefficient in a forced linear hyperbolic differential equation from the knowledge of the solution at one or more isolated points is dealt with. The continuous model of a structural system by a shear beam is used to study the utility of earthquake records in determining structural models. Starting with an initial "guess," a systematic method of iteratively improving the estimate of the structural stiffness using the information contained in the measured response to a known ground excitation is developed. A highly efficient and automatic numerical algorithm for this purpose, based on an optimal control formulation of the problem of history matching is developed. Numerical examples are presented showing the dependence of the estimate on the initial guess. The nonunicity of the estimate is demonstrated, pointing to the fact that though history matching at one or more points in a structure may be a necessary condition for arriving at an adequate model, it may not be a sufficient one.

Introduction

The increasing number of tall structures in seismically active areas all over the world has led, in recent years, to a considerable amount of interest in the determination of structural response to strong earthquake ground motions. The installation of accelerographs nowadays in various large structures has greatly increased the pool of data pertinent to structural behavior during large ground excitations (e.g., Udwadia and Trifunac [1][1]). The recent San Fernando earthquake of Feb. 9, 1971, for example, yielded about 180 acceleration histories that were recorded in building structures in the Los Angeles area (Hudson [2]). The acquisition of such data obviously holds out the possibility of obtaining improved structural models which can then in turn be used to ascertain the expected structural responses to future earthquakes. It therefore becomes important at this stage to assess critically the utility of such recordings in improving our understanding of the structural systems involved.

This paper deals with the determination or updating of a building structural model from earthquake records obtained in the structure. More specifically, it concerns the estimation of structural stiffness as a function of building height, based on noiseless measurements of structural motions at one or more levels in the structure, created by perfectly known ground inputs.

Through the problem of estimating the stiffness and damping at the various levels of a building structure has been investigated by several researchers in the past (e.g., Berg [3], Nielsen [4], Ibañez [5]), they have concentrated on data obtained from vibration tests. All the investigations so far have used lumped-parameter models and few if any have attempted a systematic estimation procedure based on earthquake recordings.

The salient feature of the technique proposed here is that the structure is considered a continuous system making the method applicable to *all* systems which can be mathematically modeled by linear hyperbolic partial differential equations. We have adopted Jennings' [6] shear beam model to represent mathematically a simple building structural system. Such a model has been shown by Jennings to be adequate in representing several tall steel as well as reinforced concrete buildings.

The simplest approach to obtaining an estimate of the structural stiffness would be to try to obtain the "closest-fit" between the history of motion measured at one or more points in the structure and the calculated response of the model at the corresponding

[1]Numbers in brackets designate References at end of paper.

Contributed by the Design Engineering Division and presented at the Design Engineering Technical Conference, Washington, D.C., September 17–19, 1975, of THE AMERICAN SOCIETY OF MECHANICAL ENGINEERS. Manuscript received at ASME Headquarters June 4, 1975. Paper No. 75-DET-77.

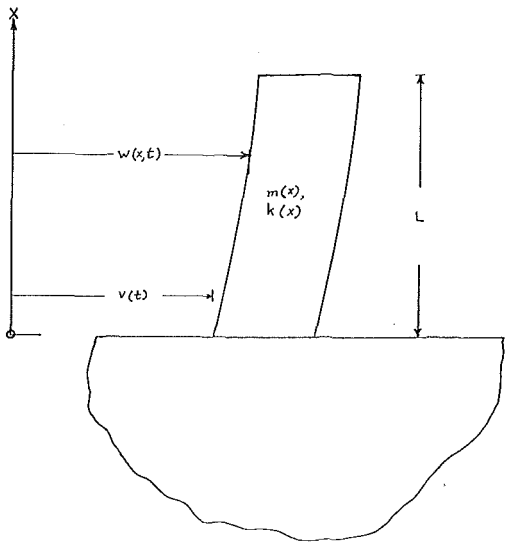

Fig. 1

points. This can be done by starting out with a suitable guess of the parameters to be estimated, by visually examining the output of each simulator run, and then adjusting one or more of the parameters by intuition or experience (e.g., Wood [7]). However, such a trial and error procedure is often very time consuming and expensive. One would like then, *in principle,* to be able to have a systematic method which does not require an inordinate amount of computation time.

An obvious method of achieving such a match of recorded and calculated responses would be to derive an iterative scheme, which, starting from an "initial guess" of the parameters, iteratively updates them so as to converge to the true values of the parameter. The commonly used procedure (Jacquard and Jain [8]) for this is to determine the so-called "sensitivity coefficients" which give the rate of change of the model response at the measurement points with respect to the parameters being estimated. These coefficients determine the way the parameter estimates need to be changed to improve successively the history match between the measured and calculated responses. However, a determination of these coefficients involves the integration of the system equations $(n + 1)$ times (where n is the number of parameters to be estimated) at each iteration making the estimation procedure very time consuming and therefore computationally inefficient. For instance, a fifty-story building if modeled by 50 lumped masses ($n = 50$) would need at *each* iteration the integration of the system equation 51 times. Considering that one may need 50 to 100 iterations, depending on the quality of one's "initial guess" for arriving at a good set of estimates, the computation times involved herein may become highly excessive.

Alternately, the computation of the sensitivity coefficients by the method similar to that suggested by Jacquard and Jain [8] and Carter et al. [9] will require $(m + 1)$ integrations of the system equation (where m is the number of observation locations) and a quadrature for evaluation of a convolution integral over the whole X space up to the observation time for each observation. This can also be easily seen to require a large amount of computation. This procedure can be made more efficient numerically by considering sensitivity coefficients corresponding to the rate of change of a single scalar criterion, J, which measures the degree of history mismatch (over the whole period of measurement) with respect to the parameters.

The method proposed here is based on an optimal control formulation of the history-matching problem. It gives the sensitivity coefficients of the scalar criterion J with respect to all the parameters in a single integration of the system equation and its adjoint, thus reducing the number of integrations required at each iteration from $n + 1$ to two. For tall buildings (large n), this would lead to a large computational economy over conventional methods of computing the gradient, especially when the number of iterations is large. A similar technique has been used by Chen et al. [10] in their identification of a parabolic partial differential equation.

Having developed this efficient algorithm, the estimation technique has been applied to the study of building structural stiffness from 'input-output' records, obtained in structures during strong ground motion. Four different numerical examples pertinent to building structures have been illustrated. The critical importance of the "initial guess" and of the input characteristics to the estimation problem is clearly brought out. The nonunicity of the estimate obtained in the solution of this inverse problem is indicated, and it is shown that though history matching at a particular level in the structure may be a necessary condition for obtaining the correct model, it is not a sufficient one.

Theory

(a) Structural Model. The "shear-beam" representation of some types of structures for purposes of studying their horizontal unidirectional vibratory characteristics has been well documented in the past (Nielsen [4], Jennings [6]). The structural model adopted here consists of a shear beam whose stiffness varies with its height, x above ground level. It will be assumed that the mass distribution $m(x)$ per unit height of the structure is known and that the stiffness distribution $k(x)$ per unit height of the structure is to be estimated from measurements at the base and one or more points elsewhere in the structure. Fig. 1 illustrates the structural system described by the equations

$$m(x)\frac{\partial^2 w}{\partial t^2} = \frac{\partial}{\partial x}\left[k(x)\frac{\partial w}{\partial x}\right] \tag{1}$$

$$w(0, t) = v(t) \tag{2}$$

$$k(x)\frac{\partial w}{\partial x}\Big|_{x=L} = 0 \tag{3}$$

where $w(x, t)$ is the total displacement at time, t, of point x of the structure measured with respect to an inertial frame of reference and $v(t)$ is the displacement history at the base of the structure. Assuming that the structure starts from rest, we have

$$\left.\begin{aligned} w(x, 0) &= 0 \\ \frac{\partial w(x, 0)}{\partial t} &= 0 \end{aligned}\right\} \tag{4}$$

The measurements are all assumed noise free and comprise of the time histories $w^{\text{obs}}(x_i, t)$; $i \in [1, m]$, $t \in [0, T]$, together with the base motion $v(t)$. Though such an assumption is often not realistic, it will help in focusing our attention to the difficulties involved in the solution of the exact inverse problem without bringing in the added complications and uncertainties involved with noisy data.

(b) Approach to the Identification Problem. The method involves iteratively changing the stiffness estimates, starting from an initial "guess" in a systematic manner so as to get successively better agreement between the measured response to a given ground motion input and the predicted model response, at the m measurement points x_i, $i = 1, \ldots, m$. The estimate $k(x)$, is then such that the positive definite functional given by

$$\hat{J} = \frac{1}{2}\sum_{i=1}^{m}\int_0^t [w^{\text{obs}}(x_i, t) - w(x_i, t)]^2 dt \tag{5}$$

is a minimum. $w^{\text{obs}}(x_i, t)$ is the measured response at point x_i and $w(x_i, t)$ is the calculated model response [equations (1) to (4)]. The minimization of $\hat{J}$ is done by a gradient algorithm essentially following the hill climbing technique.

(c) Unicity and Consequent Modification of the Error Criterion. The problem of uniqueness of the estimates obtained by the process of history matching at a few isolated points has not so far been solved and is being currently investigated. The numerical

experience of the authors suggests, however, that unicity of estimates in the unconstrained identification of the hyperbolic problem does not exist. Similar observations have been made by several authors in their discussion of parabolic partial differential equations (Chavent, [11], Chen et al. [10]). Workers in problems involving parabolic equations (Carter et al. [9]) have found, however, that putting inequality constraints on the estimated parameters give rise to better convergence characteristics by confining the estimates to a portion of the parameter space of interest. These constraints yield more feasible values of the final estimates and are based on a prior knowledge of the ranges of values that the parameters being estimated can have. However, this procedure can be unsatisfactory because, as in linear programming, the final estimates often reproduce the boundary values of the supplied constraints.

In this paper two different types of constraints have been investigated: *(a)* constraints on the magnitude of the gradient of the parameter function being estimated and *(b)* constraints on its second derivative. They were motivated by the physical requirement that the stiffness distributions change "smoothly" with height.

These constraints on the function $k(x)$, which is being estimated, are implemented by adding a penalty functional to $\bar{J}$ to give

$$J = \frac{1}{2}\sum_{i=1}^{m}\int_0^T [w^{\text{obs}}(x_i, t) - w(x_i, t)]^2 dt + \frac{a}{2}\int_0^L \left[\frac{\partial k}{\partial x}\right]^2 dx + \frac{b}{2}\int_0^L \left[\frac{\partial^2 k}{\partial x^2}\right]^2 dx \quad (6)$$

where a and b are positive weighting factors. Minimizing this functional will then lead to a history match as well as the satisfaction of the constraints by a reduction in the magnitudes of the first and second derivatives of $k(x)$. The degree of satisfaction of these constraints will naturally depend upon the relative magnitudes of the weighting factors. For instance, when $a = 0$, no penalty is levied on the magnitude of the first derivative, so that the first derivative constraint is completely relaxed.

It appears that in building estimation problems these derivative constraints are more helpful in obtaining a unique estimate than the inequality constraints. However, if a very large penalty is placed on the derivative constraint terms, it may considerably slow down the convergence of the minimization process. If, on the other hand, the function $k(x)$, for example, *does* have definite gradients for a major portion of the x-space, the constraint *(a)* may adversely affect the final identification process. From this point of view, a more useful constraint for most structural systems would then be that pertaining to the second derivative. This has been verified by our building studies presented in the following sections.

(d) Derivation of the Formula for the Gradient of J. Adjoining to J the constraint equation (1) that $w(x, t)$ must satisfy, and using a multiplier function $\Psi(x, t)$ define

$$\bar{J} = J + \int_0^L \int_0^T \Psi(x, t)\left\{m(x)\frac{\partial^2 w(x, t)}{\partial x^2} - \frac{\partial}{\partial x}\left[k(x)\frac{\partial w(x, t)}{\partial x}\right]\right\} dx\, dt \quad (7)$$

Then the first variation of $\bar{J}$ due to a variation in the estimate, $\delta k(x)$, is given by

$$\delta\bar{J} = -\int_0^L \int_0^T \sum_{i=1}^{m} [w^{\text{obs}}(x_i, t) - w(x_i t)]\, \delta w(x, t)\delta(x - x_i)\, dt\, dx + a\int_0^L \frac{\partial k}{\partial x}\cdot\frac{\partial \delta k}{\partial x}\, dx + b\int_0^L \frac{\partial^2 k}{\partial x^2}\cdot\frac{\partial^2 \delta k}{\partial x^2} dx + \int_0^L \int_0^T \Psi(x, t)\left\{m(x)\frac{\partial^2 \delta w}{\partial t^2} - \frac{\partial}{\partial x}\left[k(x)\frac{\partial \delta w}{\partial x}\right] - \frac{\partial}{\partial x}\left[\delta k(x)\frac{\partial w}{\partial x}\right]\right\} dx\, dt + \text{higher order terms} \quad (8)$$

Integrating the various terms by parts and omitting for brevity the arguments (x, t) of w and Ψ, we have

$$\int_0^L \frac{\partial k}{\partial x}\cdot\frac{\partial \delta k}{\partial x} dx = \frac{\partial k}{\partial x}\delta k(x)\Big|_0^L - \int_0^L \frac{\partial^2 k}{\partial x^2}\delta k(x)\, dx, \quad (9)$$

$$\int_0^L \frac{\partial^2 k}{\partial x^2}\cdot\frac{\partial^2 \delta k}{\partial x^2} dx = \frac{\partial^2 k}{\partial x^2}\cdot\frac{\partial \delta k}{\partial x}\Big|_0^L - \frac{\partial^3 k}{\partial x^3}\delta k(x)\Big|_0^L + \int_0^L \frac{\partial^4 k}{\partial x^4}\delta k(x)\, dx, \quad (10)$$

and

$$\int_0^L \int_0^T \Psi\left\{m(x)\frac{\partial^2 \delta w}{\partial t^2} - \frac{\partial}{\partial x}\left[k(x)\frac{\partial \delta w}{\partial x}\right] - \frac{\partial}{\partial x}\left[\delta k(x)\frac{\partial w}{\partial x}\right]\right\} dx\, dt = \int_0^L \left[\Psi m(x)\frac{\partial \delta w}{\partial t}\Big|_0^T - \frac{\partial \Psi}{\partial t}m(x)\delta w(x, t)\Big|_0^T + \int_0^T \frac{\partial^2 \Psi}{\partial t^2}m(x)\delta w\, dt\right] dx - \int_0^T \left\{\Psi k(x)\frac{\partial \delta w}{\partial x}\Big|_0^L - \frac{\partial \Psi}{\partial x}k(x)\delta w\Big|_0^L + \int_0^L \frac{\partial}{\partial x}\left[\frac{\partial \Psi}{\partial x}k(x)\right]\delta w\, dx + \Psi\delta k(x)\frac{\partial w}{\partial x}\Big|_0^L - \int_0^L \frac{\partial \Psi}{\partial x}\frac{\partial w}{\partial x}\delta k(x)\, dx\right\} dt \quad (11)$$

Using equations (8) to (11) and collecting the coefficients of $\delta k(x)$ and $\delta w(x, t)$, the variation $\delta\bar{J}$ can be expressed as

$$\delta J = a\left[\frac{\partial k}{\partial x}\delta k(x) + b\frac{\partial^2 k}{\partial x^2}\frac{\partial \delta k}{\partial x} - b\frac{\partial^3 k}{\partial x^3}\delta k(x)\right]_0^L - \int_0^L \left[\left(a\frac{\partial^2 k}{\partial x^2} - b\frac{\partial^4 k}{\partial x^4}\right) - \int_0^T \delta\frac{\partial \Psi}{\partial x}\frac{\partial w}{\partial x} dt\right]\partial k(x)\, dx + \int_0^L \left\{\Psi m(x)\frac{\partial \delta w}{\partial t}\Big|_0^T - \frac{\partial \Psi}{\partial t}(x, t)m(x)\delta w\Big|_0^T\right\} dx - \int_0^T \left\{\Psi k(x)\frac{\partial \delta w}{\partial x}\Big|_0^L - \frac{\partial \Psi}{\partial x}k(x)\delta w\Big|_0^L + \Psi\delta k(x)\frac{\partial w}{\partial x}\Big|_0^L\right\} dt + \int_0^L \int_0^T \left\{\frac{\partial^2 \Psi}{\partial t^2}m(x) - \frac{\partial}{\partial x}\left[k(x)\frac{\partial \Psi}{\partial x}\right] - \sum_{i=1}^{m}[w^{\text{obs}}(x_i, t) - w(x_i, t)]\,\delta(x - x_i)\right\}\delta w\, dx\, dt \quad (12)$$

Variations on equations (2), (3), and (4) similarly lead to the relations

$$\delta w(0, t) = 0 \quad (13)$$

$$k(L)\frac{\partial \delta w}{\partial x}\Big|_{x=L} + \delta k(L)\frac{\partial w}{\partial x}\Big|_{x=L} = 0 \quad (14)$$

and

$$\left.\begin{aligned}\delta w(x, 0) &= 0\\ \frac{\partial \delta w}{\partial t}(x, 0) &= 0\end{aligned}\right\} \quad (15)$$

respectively. If now the function $\Psi(x, t)$ is restricted such that

$$m(x)\frac{\partial^2 \Psi}{\partial t^2} = \frac{\partial}{\partial x}\left[k(x)\frac{\partial \Psi}{\partial x}\right] + \sum_{i=1}^{m}[w^{\text{obs}}(x_i, t) - w(x_i, t)]\,\delta(x - x_i) \quad (16)$$

and

$$\Psi(x, T) = 0, \quad (17)$$

$$\frac{\partial \Psi}{\partial l}(x, T) = 0, \quad (18)$$

$$\Psi(0, t) = 0, \text{ and} \quad (19)$$

$$k(L)\frac{\partial \Psi}{\partial x}(L, t) = 0, \quad (20)$$

then equation (12) reduces to

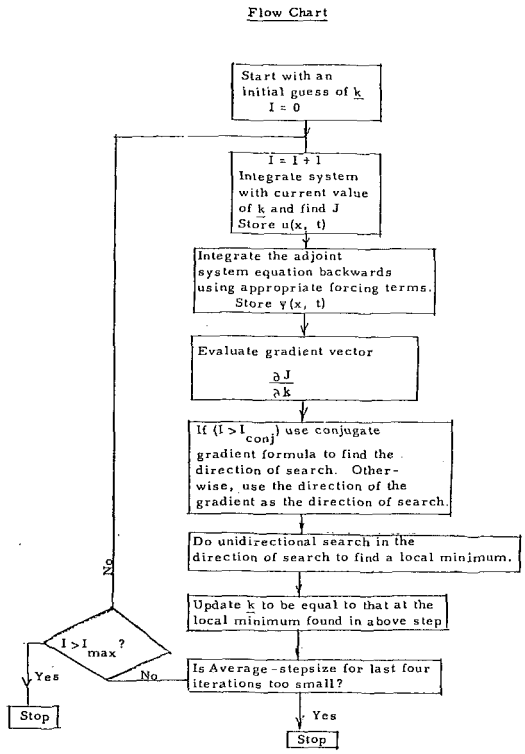

Fig. 2

$$\delta\bar{J} = \left[a\frac{\partial k}{\partial x} - b\frac{\partial^3 k}{\partial x^3}\right]\delta k(x)\Big|_0^L + b\frac{\partial^2 k}{\partial x^2}\frac{\partial \delta k}{\partial x}\Big|_0^L - \int_0^L \left[a\frac{\partial^2 k}{\partial x^2} - b\frac{\partial^4 k}{\partial x^4} - \int_0^T \frac{\partial \Psi}{\partial x}\frac{\partial w}{\partial x}dt\right]\delta k(x)\,dx \quad (21)$$

It may be noted that equations (16) to (20) define an initial value problem with point sources and appropriate boundary conditions and, hence, define $\Psi(x, t)$ uniquely. Having found Ψ, the derivative of J with respect to $k(x)$ can be determined from equation (21).

Since $\delta\bar{J} = \delta J$ if $w(x, t)$ satisfies the system equations (1) to (4), we have

$$\begin{aligned}\delta J &= \int_0^L \left[\left\{\left[a\frac{\partial k}{\partial x} - b\frac{\partial^3 k}{\partial x^3}\right][\delta(x-L) - \delta(x)] - a\frac{\partial^2 k}{\partial x^2} + b\frac{\partial^4 k}{\partial x^4} + \int_0^T \frac{\partial \Psi}{\partial x}\frac{\partial w}{\partial x}dt\right\}\delta k(x) + b\frac{\partial^2 k}{\partial x^2}\frac{\partial \delta k}{\partial x}[\delta(x-L) - \delta(x)]\right]dx \\ &= \int_0^L \left\{\left[a\frac{\partial k}{\partial x} - 2b\frac{\partial^3 k}{\partial x^3} + b\frac{\partial^2 k}{\partial x^2}\right][\delta(x-L) - \delta(x)] - b\frac{\partial^2 k}{\partial x^2}[\delta'(x-L) - \delta'(x)] - a\frac{\partial^2 k}{\partial x^2} + b\frac{\partial^4 k}{\partial x^4} + \int_0^T \frac{\partial \Psi}{\partial x}\frac{\partial w}{\partial x}dt\right\}\delta k(x)\,dt \quad (22)\end{aligned}$$

Then, the functional derivative of J with respect to the function $k(x)$ is given by

$$\frac{\delta J}{\delta k(x)} = a\frac{\partial k}{\partial x} - 2b\frac{\partial^3 k}{\partial x^3} + b\frac{\partial^2 k}{\partial x^2}[\delta(x-L) - \delta(x)] - b\frac{\partial^2 k}{\partial x^2}[\delta'(x-L) - \delta'(x)] - a\frac{\partial^2 k}{\partial x^2} + b\frac{\partial^4 k}{\partial x^4} + \int_0^T \frac{\partial \Psi}{\partial x}\frac{\partial w}{\partial x}dt \quad (23)$$

For numerical computations it will not be necessary to use equation (23), because when working with the discritized version, equation (21) can be directly utilized.

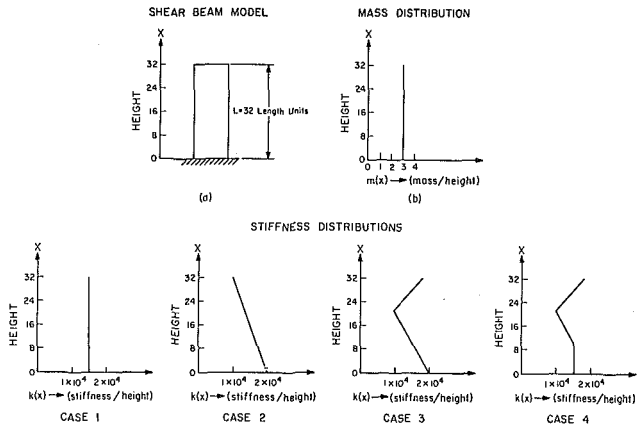

Fig. 3

Algorithm

The minimization of the error criterion, J, is done by the hill climbing technique. As it is not possible to work computationally with an infinite dimensional function $k(x)$, an appropriate discretization of $k(x)$ by a set of N values of k at the various node points was done. Such a discretization leads to J being a positive definite function in N dimensional k-space. The minimization of J is then effected by climbing down this N dimensional hypersurface taking, at each stage, a step in the direction of the local negative gradient of J with respect to the N component vector $\mathbf{k}$ calculated using equations (21) to (23).

As is well known, the rate of convergence of a gradient algorithm is often considerably enhanced, without much increase in computational load, by the use of the conjugate gradient algorithm (Polak, 1973). However, this algorithm being designed for nearly quadratic functions was not found to perform well when the model parameters were greatly different from their actual values, the functional J, in those cases, being far from a quadratic surface in the parameters to be estimated. Hence, the method of steepest descent was used in the initial phases of the estimation process. Later on, the iterations were performed using the conjugate gradient algorithm in order to get improved convergence characteristics.

The unidirectional search at each iteration consisted of evaluating $J(\mathbf{k})$ at the starting point of each iteration, $\mathbf{k}_0$, and at two equidistant points, $\mathbf{k}_1$ and $\mathbf{k}_2$, in the direction of the negative gradient as obtained by equation (21) (or in the search direction when using the conjugate gradient method). The distance between the successive points was taken to be the current search-step size. Next, the derivative of J at $\mathbf{k}_0$ in the search direction was evaluated by projection of the gradient in the search direction. This derivative together with the values of J evaluated at points $\mathbf{k}_0$, $\mathbf{k}_1$, and $\mathbf{k}_2$ were used to determine if the minimum of J fell beyond the three points or between the first point ($\mathbf{k}_0$) and the third point ($\mathbf{k}_2$). If the minimum fell beyond $\mathbf{k}_2$, additional steps were taken until three successive values of J indicated the presence of a local minimum between them. If the minimum fell between $\mathbf{k}_0$ and $\mathbf{k}_1$, the steps were successively halved until a local minimum was indicated between three successive points by three successive values of J. A parabola was next fitted between the three points and the minimum point taken to be that of the parabola. The search step was set at the beginning of each iteration to be equal to the average of the actual steps resulting in the last four iterations. This was done to keep the number of evaluations of J small. Fig. 2 shows a summary flow chart of the algorithm used.

Application and Numerical Results

As the determination of the mass distribution in a structure is in general more tractable from general engineering data than the distribution of structural stiffness, it has been assumed that the mass

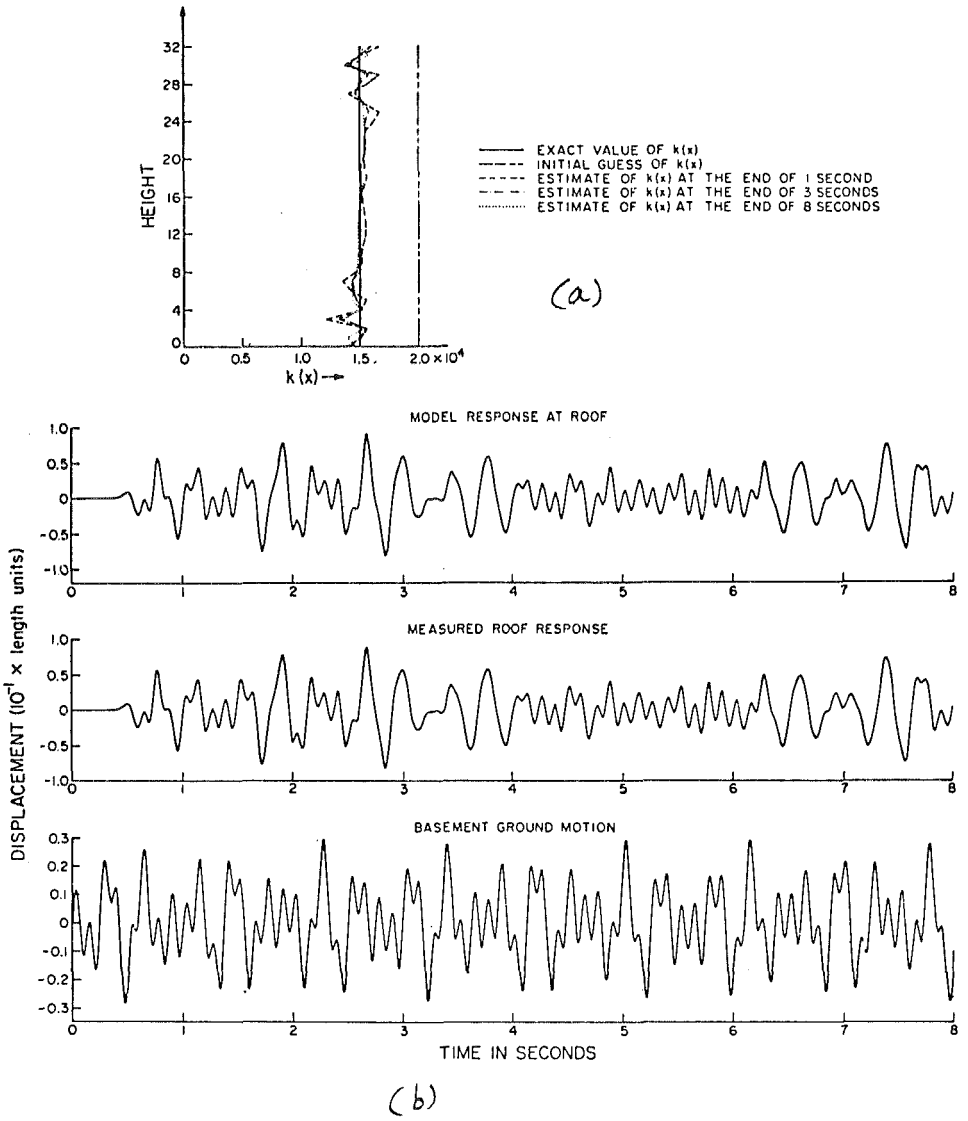

Fig. 4

distribution is perfectly known and that the identification of the stiffness based on response records is required. However, it may be pointed out that the approach taken here can be easily extended to allow a simultaneous estimation of both $m(x)$ and $k(x)$. In view of the level of accuracy to which $m(x)$ is generally known, the high computational costs involved in making a multifunction search, and the possibility of a more severe lack of unicity, this has not been done here. Further, soil structure interaction has been neglected and the structure is assumed to respond as a shear beam on a rigid foundation.

Fig. 3 shows the building structure modeled as a shear beam having a constant mass distribution all along its height. The effectiveness of the identification scheme proposed here is studied as applied to four different types of stiffness distributions, $k(x)$, indicated in Fig. 3*(c)* by the plots of stiffness/unit height as a function of the building height, x. Case 1 corresponds to a constant stiffness distribution all along the height of the structure (Fig. 3). The mass and stiffness values are chosen such that the fundamental period of the structure is 1.8 sec, corresponding to say a 16 to 20 story building. Case 2 refers to a linearly reducing stiffness. Case 3 and Case 4 have 'notch' shaped distributions wherein the stiffness decreases up to a certain height and then increases [Fig. 3*(c)*]. Such situations could be caused by the weakening of local areas along the height of the structure due to earthquake damage.

Using these exact stiffness distributions indicated in the four cases, a numerical integration of equations (1) to (4), for known inputs, yielded the "measured" displacement response at the roof of the structure.

For purposes of integration the height L was discretized into 32 equal segments of the unit length. This reduces the function $k(x)$ to a 33 parameter vector, each component of which is the value of $k(x)$ at each of the 33 grid points. Time was discretized in steps, Δt. To ensure unconditional stability in the integration of the partial differential equation, an "implicit scheme" was used in which the space derivatives occurring on the right hand side of equation (1) were taken as their time averages calculated over the earliest and latest times occurring in the discretization of the time derivative on the left hand side of the equation (Fox, 1962).

The input ground motions were constructed as a sum of four sinusoids (Δt = 0.01 sec) of various frequencies [Figs. 4*(b)*, 5*(b)*, 6*(b)*, 7*(b)*, 8*(b)* and 9*(b)*] and are fairly representative of close-in earthquake type ground excitations. Figs. 10*(b)* and 11*(b)* (Δt = 0.05 sec) show 30 sec of the El Centro Earthquake, 1940, NS component of ground displacement also used as inputs for identification purposes. These computed roof motions were then assumed to be the "measurements," and the inputs to be the recorded ground shaking. These input-response histories were next used to estimate the stiffness distribution (using the scheme resulting from the optimal control

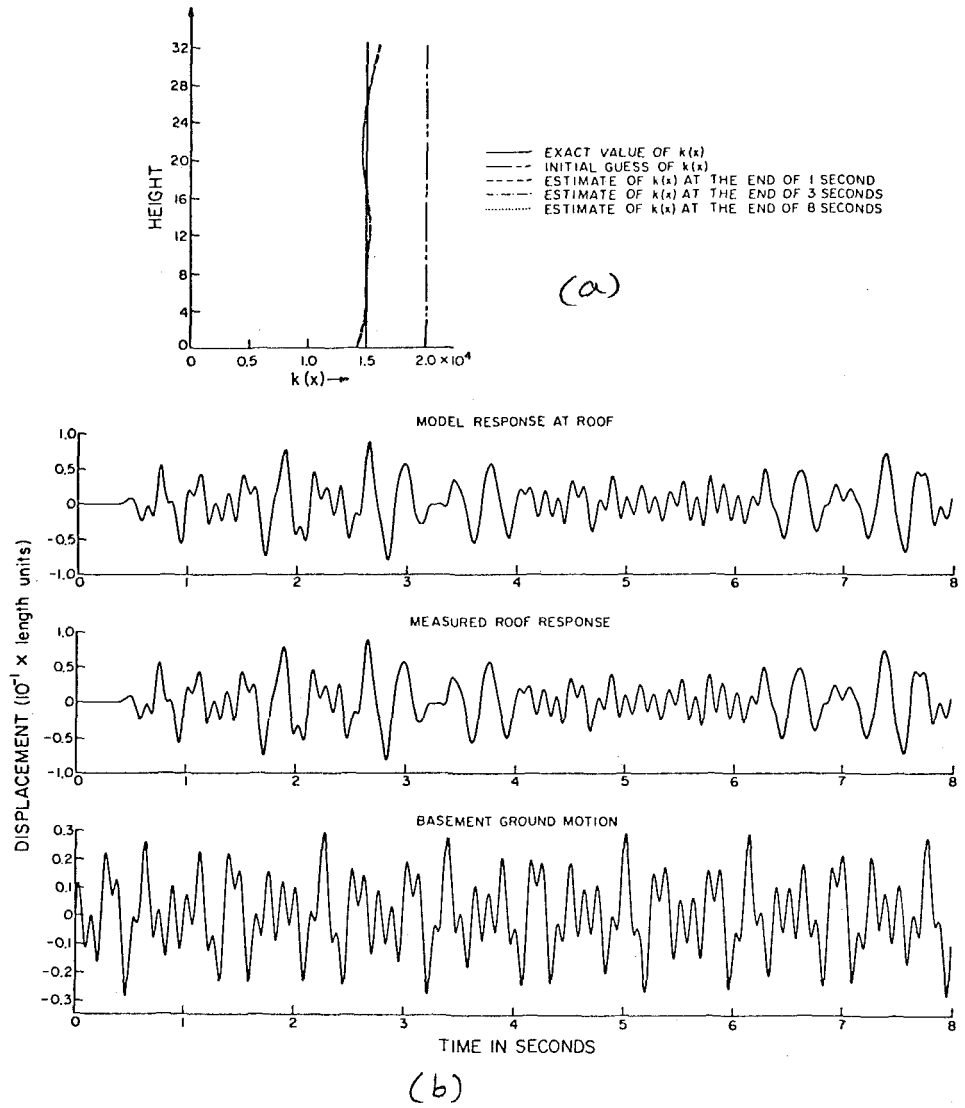

Fig. 5

formulation of the history matching problem) starting with various initial "guess distributions." The final estimates were then compared with the exact values in each of the four cases.

Fig. 4*(a)* shows the exact values of $k(x)$ (thick line), the starting guess of $k(x)$ (- -), and the estimates of $k(x)$ for various time lengths of record used in the identification. The initial guess was taken to be a constant with respect to height. The input basement motions, the "measured response" and the model response for the stiffness distribution arrived at, using an 8 sec length of time history, are indicated in Fig. 4*(b)*. As seen in the figure the history match is excellent. The values of $k(x)$ obtained at the end of 8 sec of identification are very close to the exact values.

It was observed that when starting with an initial guess quite far from the exact value, the convergence was very slow and, hence, computationally expensive if a long record of measurements was used for history matching. The computational effort was further increased because at each iteration the equations had to be integrated over a longer time period. To reduce the computation times,

Table 1*

Time Length of Record Analyzed	Normalized Mean Error in Estimate[1]	Normalized Standard Dev. of Error in Estimate[2]	Normalized R.M.S. Error in Estimate[3]	Mean Error in Displacement History Match at Roof[4]	Standard Dev. of Error in History Match at Roof[5]	Weighting Factor of Second Derivative Penalty
INITIAL GUESS						
(0 sec)	33%	0%	33%	0.91×10^{-3}	0.27×10^{-1}	
1 sec	0.93%	6.17%	6.24%	0.4×10^{-4}	0.24×10^{-3}	0.2×10^{-9}
3 secs.	0.42%	3.77%	3.79%	0.85×10^{-5}	0.36×10^{-3}	0.6×10^{-9}
8 secs.	-0.04%	3.08%	3.08%	-0.46×10^{-5}	0.57×10^{-3}	0.16×10^{-8}

* Tabulated quantities are defined in Appendix I.

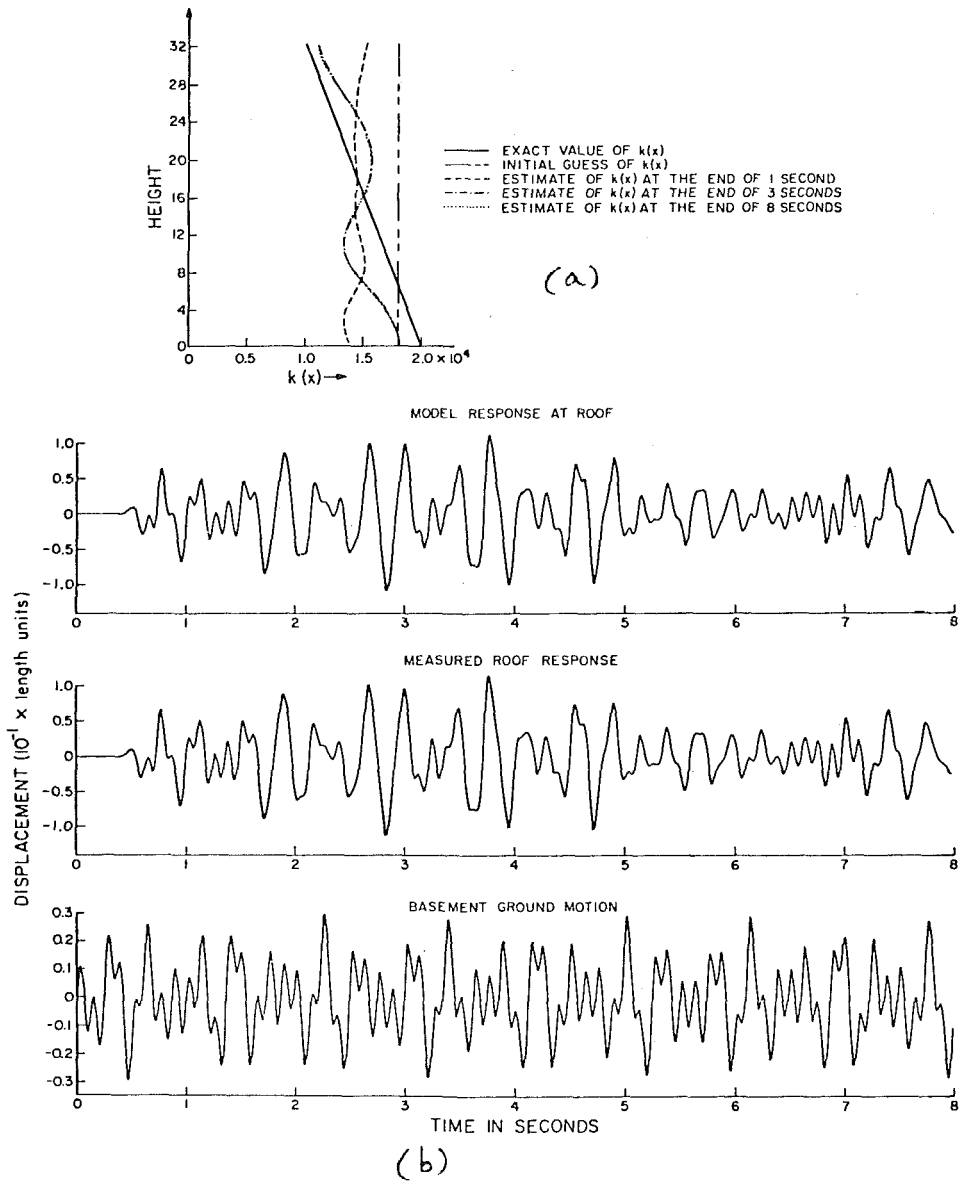

Fig. 6

1 sec of data was first processed, updating the value of $k(x)$ by obtaining a good history match for that duration. This updated estimate of $k(x)$ was next used as an initial guess for analyzing a 3 sec data length obtaining thus a new estimate of $k(x)$. The 3 sec estimate was then used as an initial guess in analyzing the entire 8 sec length of record, thus leading to a faster convergence. Fig. 4*(a)* shows the estimate of $k(x)$ so obtained at the end of 1 sec (- - -), 3 sec (-- --) and 8 sec (· · · · ·) of analysis.

The convergence to the correct values was found to largely depend on the values chosen for the initial guesses. Starting guesses which were both higher and lower than the exact values were chosen. It was found that for the constant stiffness case and the linearly varying stiffness case [Cases 1 and 2, Fig. 3*(c)*], the convergence was either very slow or nonexistent when the starting guess was higher than the mean value of the exact distribution, by more than 45 percent. Starting with these 'higher' initial guesses, the

Table 2

Time Length of Record Analyzed	Normalized Mean Error in Estimate[1]	Normalized Standard Dev. of Error in Estimate[2]	Normalized R. M. S. Error in Estimate[3]	Mean Error in Displacement History Match at Roof[4]	Standard Dev. of Error in History Match at Roof[5]	Weighting Factor of Second Derivative Penalty
INITIAL ESTIMATE (0 sec.)	33%	0%	33%	0.91×10^{-3}	0.27×10^{-1}	
1 sec.	0.24%	2.76%	2.77%	-0.7×10^{-4}	0.57×10^{-3}	0.1×10^{-8}
3 secs.	0.26%	2.59%	2.6%	-0.48×10^{-6}	0.81×10^{-3}	0.3×10^{-8}
8 secs.	0.22%	2.48%	2.49%	-0.46×10^{-5}	0.1×10^{-2}	0.8×10^{-8}

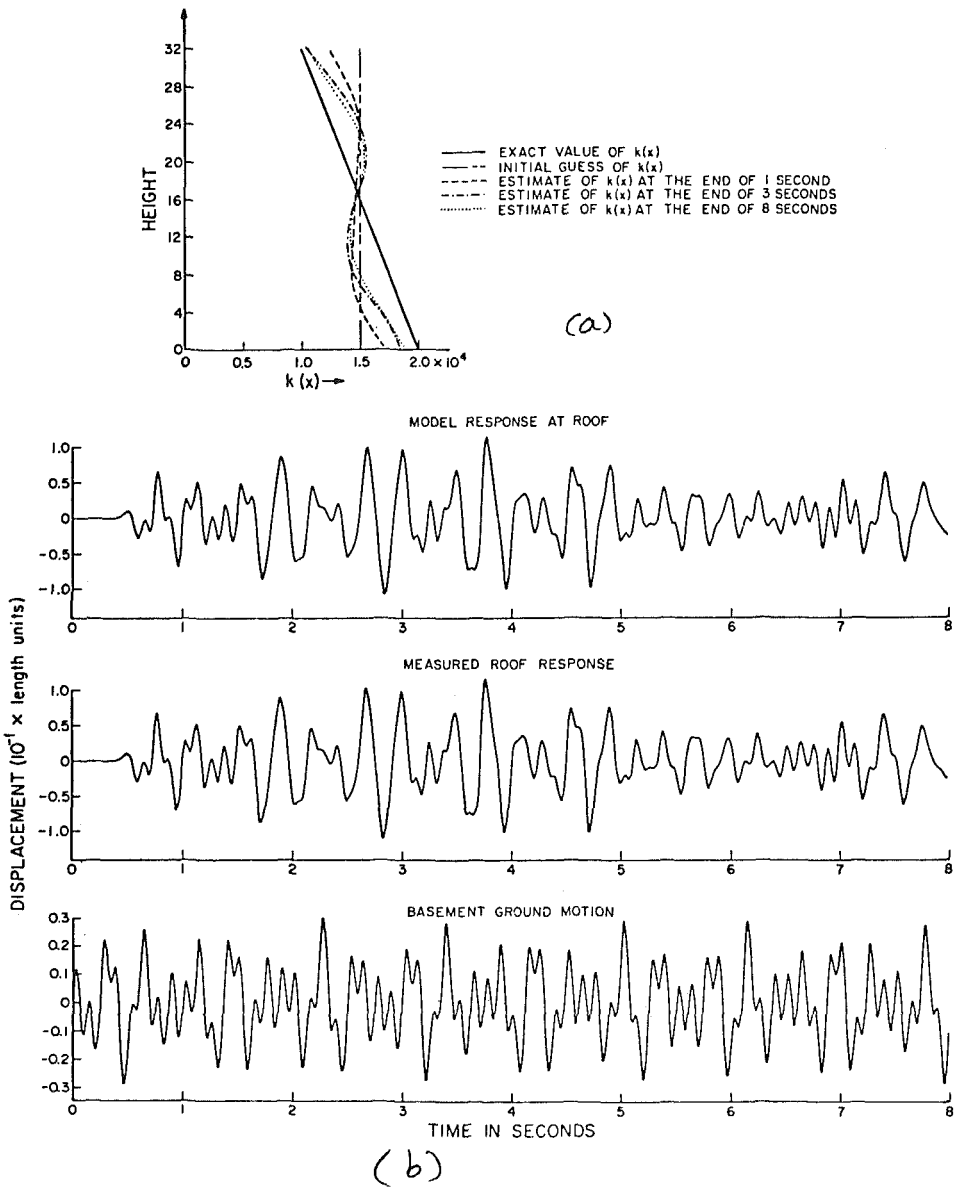

FIG. 7

history matching process for a 1 sec record duration was found to lead in all cases [Fig. 3*c*)] studied in this paper to an updated value of $k(x)$ corresponding to an approximately constant distribution lying close to the mean value of the exact stiffness distribution. Using this updated value of $k(x)$, 3 and 8 sec records were sequentially processed leading to a quick convergence. For a study of initial guesses lower than the actual values, a 1 sec record of data was processed. If the updated estimate lay close to the true mean value, the attempt was taken to be successful, since the use of such an update in the subsequent analysis of longer records always showed convergence. For Cases 1 and 2 [Fig. 3(*c*)] no convergence occurred if the initial guess was lower than the mean value of the exact distribution by more than 35 percent.

Cases 3 and 4 [Fig. 3*(c)*] with notched distributions were found to tolerate smaller errors in the initial guesses for adequate convergence and did not converge for initial guesses higher than 140 percent and lower than 80 percent of the exact mean.

Despite the close history match observed in Fig. 4*(b)*, the esti-

Table 3

Time Length of Record Analyzed	Normalized Mean Error in Estimate[1]	Normalized Standard Dev. of Error in Estimate[2]	Normalized R.M.S. Error in Estimate[3]	Mean Error in Displacement History Match at Roof[4]	Standard Dev. of Error in History Match at Roof[5]	Weighting Factor of Second Derivative Penalty
INITIAL GUESS						
(0 secs.)	20.0%	19.8%	28.1%	-0.1×10^{-2}	0.26×10^{-1}	
1 sec.	-3.4%	21.53%	21.8%	-0.6×10^{-3}	0.5×10^{-2}	0.1×10^{-10}
3 secs.	-1.6%	13.57%	13.66%	0.35×10^{-4}	0.15×10^{-2}	0.3×10^{-10}
8 secs	-1.61%	13.56%	13.6%	-0.26×10^{-4}	0.2×10^{-2}	0.8×10^{-10}

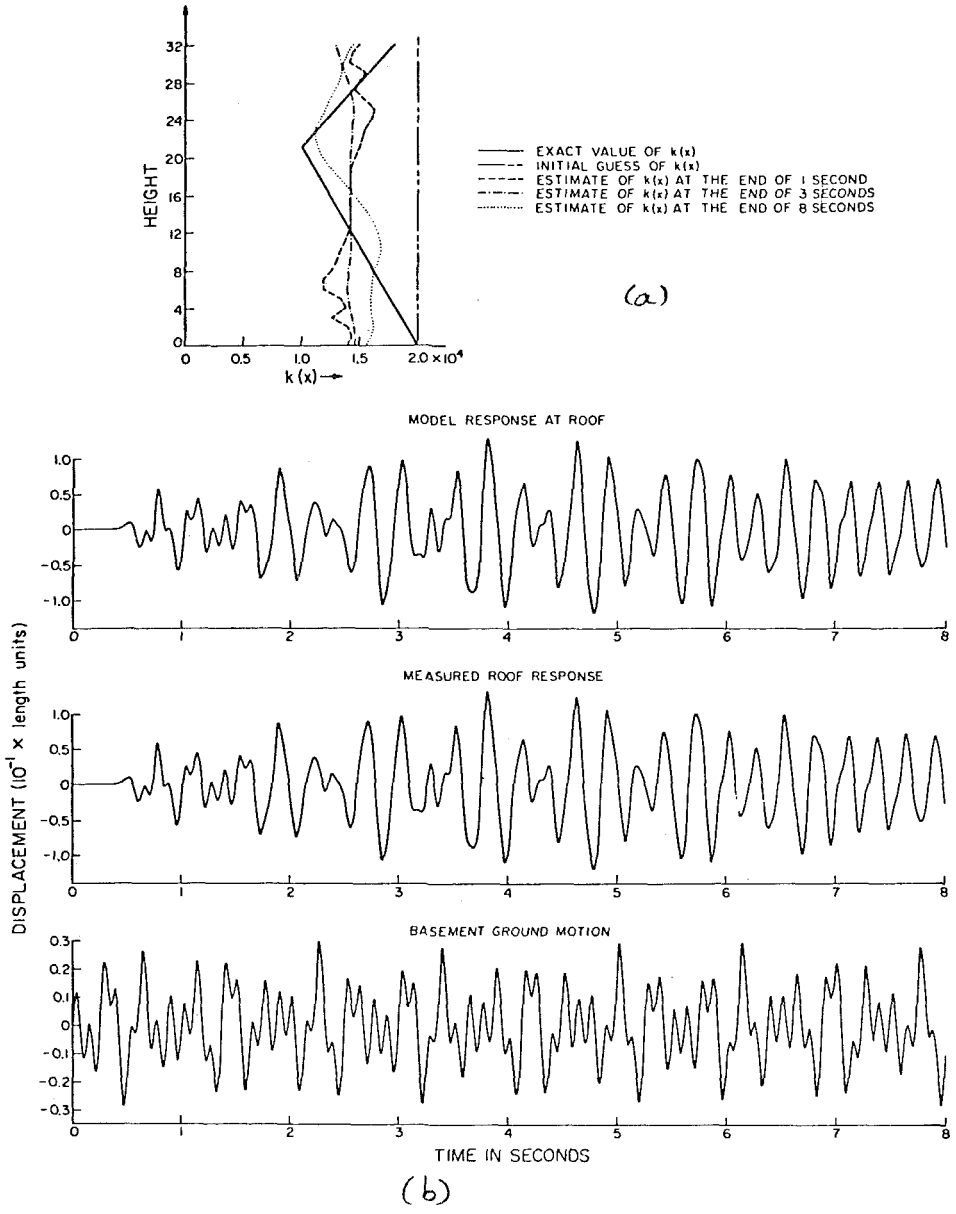

Fig. 8

mate of $k(x)$ [Fig. 4(*a*)] shows an oscillatory behavior near the top and bottom of the shear beam. This history matching here was done under the constraint that the first derivative of $k(x)$ be as small as possible all over the x domain. The first derivative penalty term was imposed in minimizing J by using a positive coefficient, a, in equation (6) and setting b equal to zero. Figs. 5(*a*) and 5(*b*) show the results of placing a constraint on the second derivative of $k(x)$ (implemented by setting $a = 0$ and b equal to a positive quantity). Fig. 5(*b*), while indicating the same quality of history match as Fig. 4(*b*), shows that the zig-zag nature of the stiffness estimate has been substantially controlled. The value of b used in the definition of the functional J, however, needs to be carefully chosen. Too large a value would slow down the convergence of the history matching process substantially, while too small a value would lead to oscillatory estimates. A little experimentation was needed before satisfactory balance between the gradient penalty

Table 4

Time Length of Record Analyzed	Normalized Mean Error in Estimate[1]	Normalized Standard Dev. of Error in Estimate[2]	Normalized R.M.S. Error in Estimate[3]	Mean Error in Displacement History Match at Roof[4]	Standard Dev. of Error in History Match at Roof[5]	Weighting Factor of Second Derivative Penalty
INITIAL GUESS						
(0 sec.)	0%	19.8%	19.8%	-0.43×10^{-3}	0.52×10^{-2}	
1 sec.	-2.64%	16.19%	16.40%	-0.2×10^{-3}	0.2×10^{-3}	0.5×10^{-8}
3 secs.	-2.44%	12.8%	13.02%	-0.36×10^{-5}	0.17×10^{-2}	0.15×10^{-7}
8 secs.	-1.88%	11.12%	11.28%	-0.24×10^{-4}	0.13×10^{-2}	0.4×10^{-7}

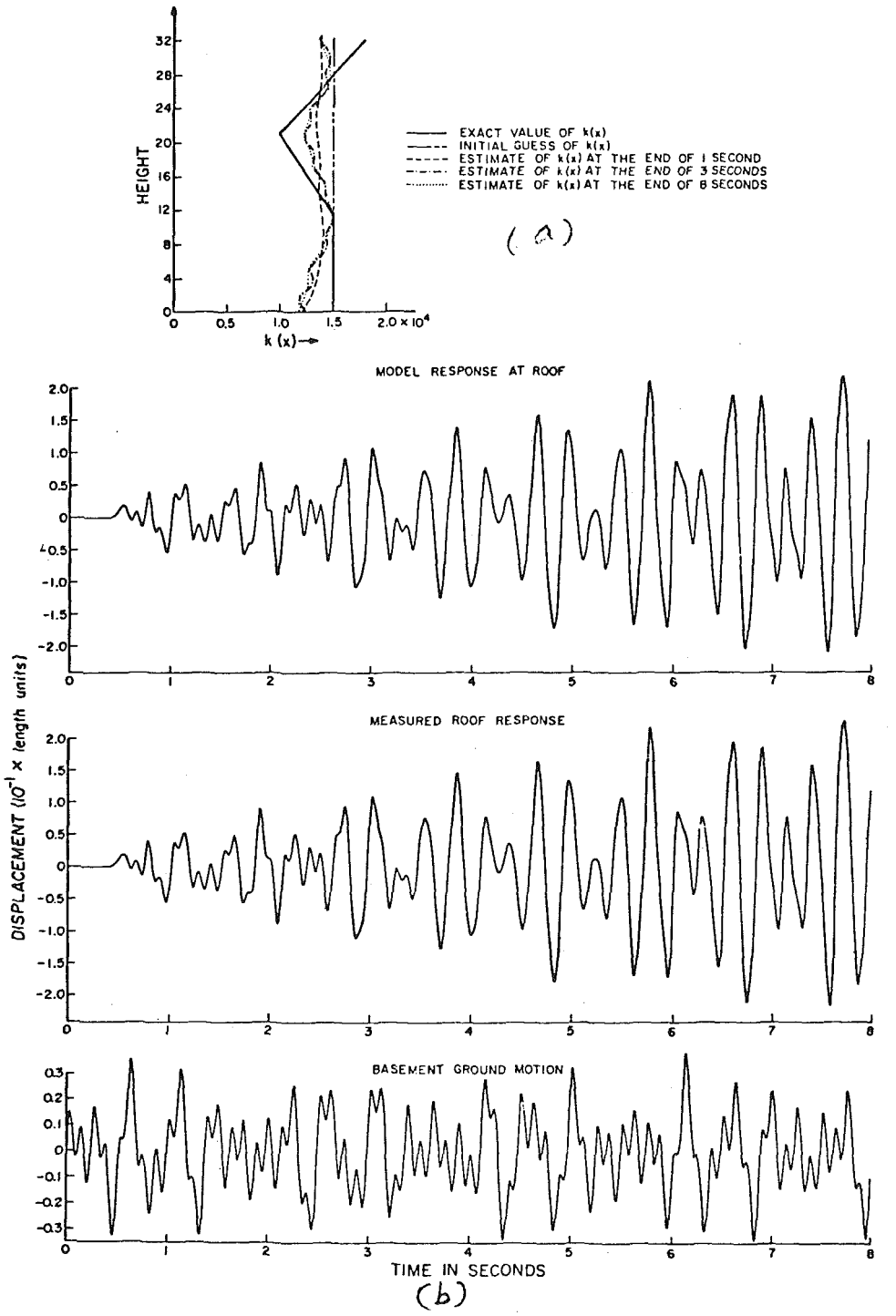

Fig. 9

terms and the history mismatch terms in functional J (equation 6) was achieved. The value of b was required to be increased in direct proportion to the length of record analyzed. For all subsequent work presented in this paper, the second derivative penalty was adopted with $a = 0$ and $b \neq 0$ (equation 6).

Table 1 summarizes the results of the estimation scheme applied to the constant stiffness case using the first derivative penalty ($a \neq 0$, $b = 0$) term in J. The initial guess was 33 percent higher than the exact value; after processing 1 sec of data, the normalized mean value (Table 1) reduced to less than 1 percent and the normalized standard deviation to about 6.2 percent. Processing of longer and longer lengths of record reduced the errors. After 8 sec of applying the identification technique with the first derivative penalty, the normalized mean error reduced to −0.04 percent and the standard deviation to 3.08 percent. The results of applying the second derivative penalty ($a = 0$, $b \neq 0$) are shown in Table 2. Though the mean error in estimated stiffness is slightly larger in Table 2 than in Table 1, the standard deviations are smaller, indicating a smoother and therefore better overall estimation.

Tabulated are also the statistics of errors in history matching over various record lengths. The standard deviations of these errors increase in each table from the result of the 3 sec to the result

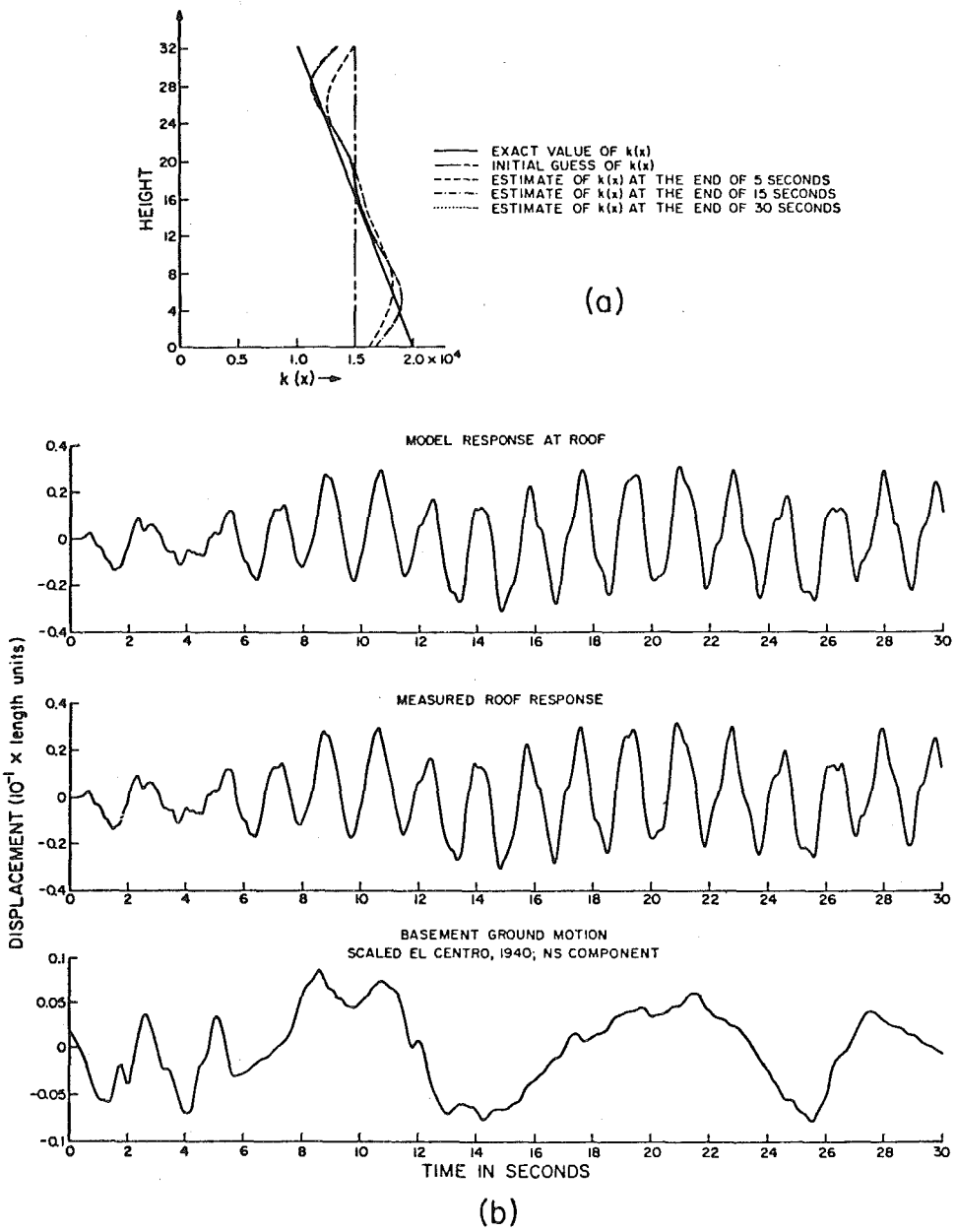

Fig. 10

of the 8 sec record lengths. In spite of the apparent worsening of the quality of history match of the latter case compared to the former, the results of 8 sec record length analysis represent an improvement on those of the 3 sec run. This is because the quality of the history match for an 8 sec record length using the estimates of a 3 sec run are much worse than that of the history match for 8 sec using the final estimates of the 8 sec run. Thus, the amount of information extracted in the latter case is larger than in the former case. The quality of history match [Figs. 4*(b)* and 5*(b)*] is nonetheless excellent. Average history match error is 2–3 percent of the

Table 5

Time Length of Record Analyzed	Normalized Mean Error in Estimate[1]	Normalized Standard Dev. of Error in Estimate[2]	Normalized R. M. S. Error in Estimate[3]	Mean Error in Displacement History Match at Roof[4]	Standard Dev. of Error in History Match at Roof[5]	Weighting Factor of Second Derivative Penalty
INITIAL GUESS (0 secs.)	35.25%	19.05%	40.06%	0.87×10^{-3}	0.28×10^{-1}	
1 sec.	-3.52%	23.11%	23.38%	0.37×10^{-4}	0.4×10^{-3}	0.4×10^{-8}
3 secs.	-4.18%	19.6%	20.08%	0.1×10^{-4}	0.15×10^{-3}	1.2×10^{-8}
8 secs.	-2.27%	14.0%	14.17%	0.73×10^{-6}	0.96×10^{-3}	3.2×10^{-8}

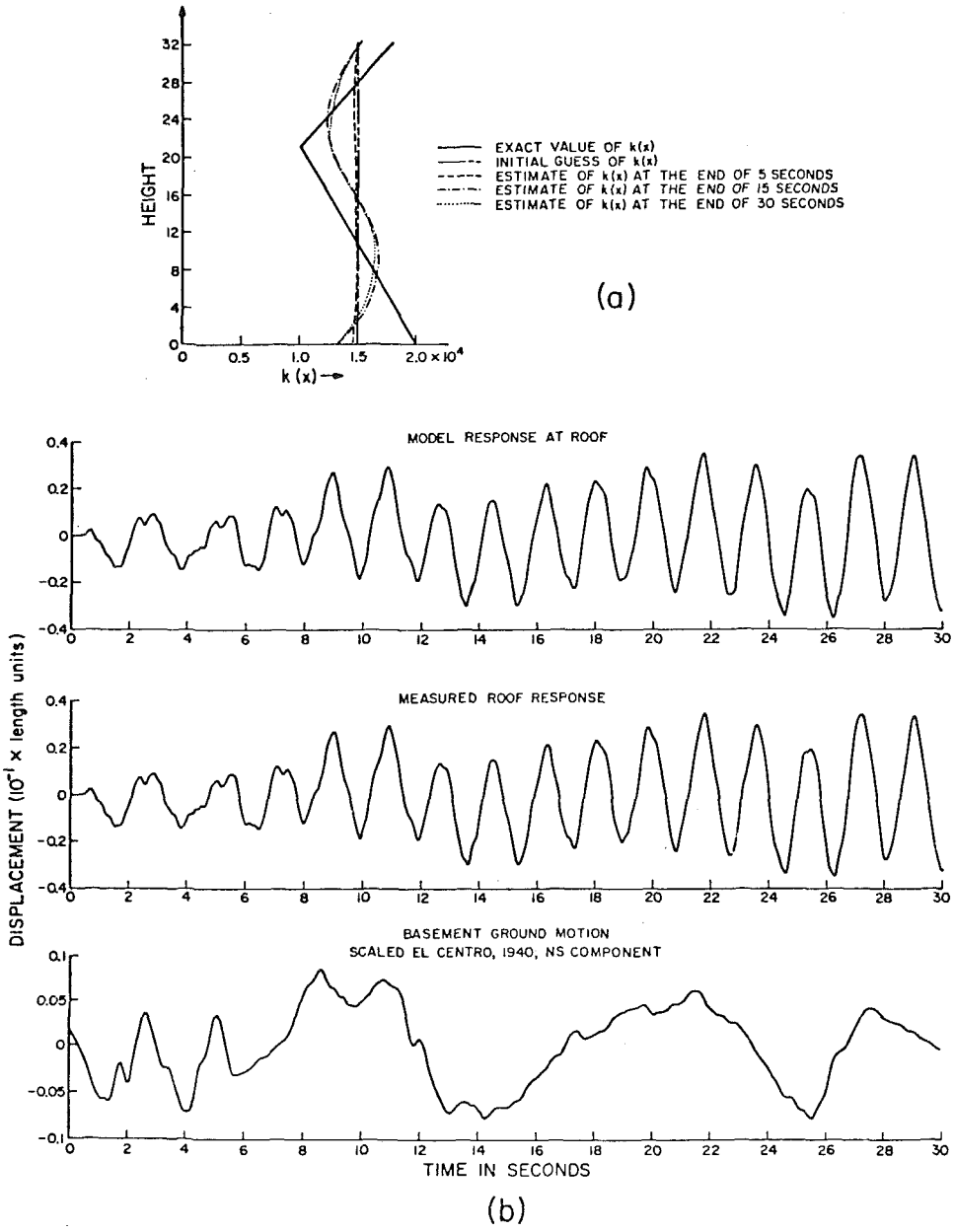

Fig. 11

rms measured displacement.

Figs. 6 and 7 (Tables 3 and 4) indicate the estimation carried out for Case 2 [Fig. 3*(c)*] corresponding to a linearly decreasing stiffness, for two initial guesses. The history matching procedure, for 1 sec, gives a good estimate of the mean stiffness [Fig. 6*(a)*], though the standard deviation is slightly increased (Table 3). However, a reduction in the mean error here represents a better estimate than the initial guess, as the estimates are now scattered more evenly about the true mean value. This is clearly brought out by the plots of the estimates at various stages of the identification process [Fig.

Table 6

Time Length of Record Analyzed	Normalized Mean Error in Estimate[1]	Normalized Standard Dev. of Error in Estimate[2]	Normalized R. M. S. Error in Estimate[3]	Mean Error in Displacement History Match at Roof[4]	Standard Dev. of Error in History Match at Roof[5]	Weighting Factor of Second Derivative Penalty
INITIAL GUESS						
(0 sec.)	7.18%	14.19%	15.9%	0.4×10^{-3}	0.12×10^{-1}	
1 sec.	-2.71%	14.12%	14.38%	0.74×10^{-4}	0.27×10^{-3}	0.8×10^{-10}
3 secs.	-2.88%	13.42%	13.73%	0.97×10^{-4}	0.146×10^{-2}	2.4×10^{-10}
8 secs.	-2.68%	13.16%	13.43%	0.116×10^{-3}	0.249×10^{-2}	3.2×10^{-10}

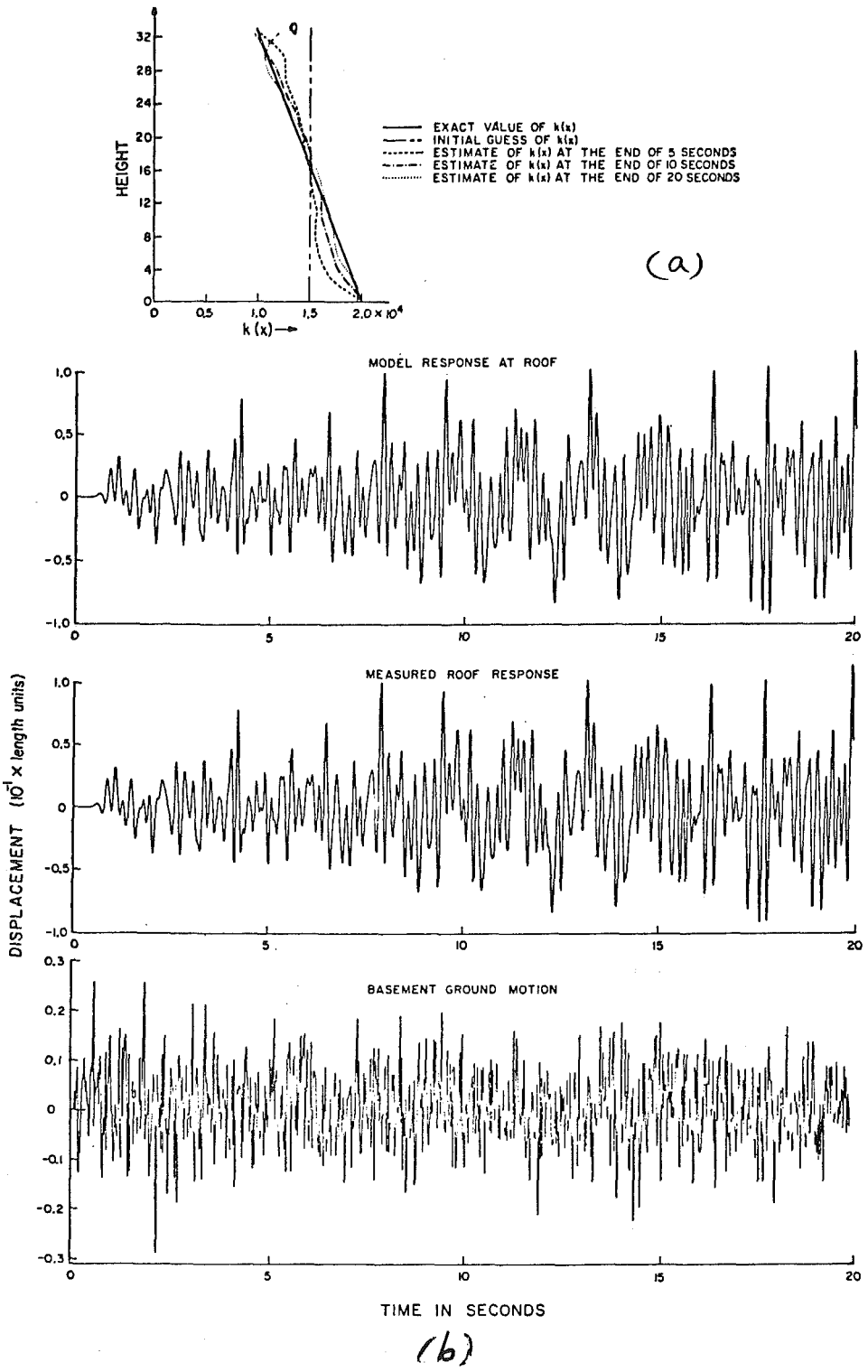

Fig. 12

5(*a*)]. A comparison of Figs. 6(*a*) and 7(*a*) indicates that, though the convergence may be slightly slower in the case where the initial guess is further off from the true mean value, the results obtained in the two cases are very similar. Again, the history match between the model and 'measured' response is very good for both initial guesses.

Figs. 8 and 9 (Tables 5 and 6) summarize the results for Cases 3 and 4 [Fig. 3(*c*)] where the true stiffness distributions are more complex and exhibit a 'notch' shaped feature. Though the normalized errors (Tables 5 and 6) are small, the standard deviations of the estimate errors are large. Fig. 8 shows that the identification scheme has been able to recover the notch-like behavior in the upper region of the structure. However, in the lower regions, the stiffness estimates are poor. This is due to the fact that inverse problem of estimation posed here is insensitive to the actual values of the stiffnesses around the base of the structure. Improved esti-

mates in these parts of the structure may require measurements at several points along the height, in addition to measurements at the roof. Fig. 9 shows similar features indicating that the estimation of building stiffness from input output records may become extremely difficult for complex distributions. Despite the excellent history match observed between the "measured" and the model response, the estimates of the stiffness are very poor.

This lack of sensitivity of the structural roof response recorded over the 8 sec duration is extremely significant, for it clearly indicates the inherent nonuniqueness underlying the estimation problem and demonstrates that history matching even under noiseless measurement conditions may not be a sufficient condition for determining the stiffness distribution in a structure. Some recent results in nonuniqueness have been obtained in reference (13).

Dependence of Stiffness Estimate on Ground Input

In addition to the dependence on the initial guess and the number of measurement points in the structure, the nature of ground input appears to be highly instrumental in determining the degree of success achievable in the identification process.

As demonstrated in Figs. 4*(a)* to 9*(a)*, there is little change in the stiffness estimates obtained in going from an analysis of a 3 sec record length to an 8 sec record length. This lack of improvement in the stiffness distribution indicates that the additional amount of information about the stiffness available from an analysis of the additional 5 sec length of data, beyond 3 sec, is negligible. This is a consequence of the fact that the input data is composed of four sinusoids and is, therefore, not broad band. For such narrow band ground input, then, beyond a certain time length no additional information is gained by an analysis of longer and longer record lengths. Ground motions generated by distant earthquakes comprise, in the main, long period surface waves. The high frequency waves get attenuated faster because of material damping through the earth media. Also, attenuation due to geometric spreading occurs. Such ground inputs would have a narrow band nature making the above discussion on their information content from the viewpoint of building identification, applicable.

Close-in ground motions, on the other hand, tend to be richer in various frequency contents and, hence, may provide inputs which are more conducive to better identification. Figs. 10 and 11 (Tables 7 and 8) show the identification carried out using the El Centro 1940, NS displacement record ($\Delta t = 0.05$ sec). The estimates look better than those obtained in Figs. 7 and 8. However, the edge effects at the boundaries are quite marked. Despite the close distance (15 km) of the recording station from the fault, the ground motion shows a strong predominance in the low frequencies.

For waves to "feel" the local changes in building stiffness, their wavelengths must be comparable to or shorter than the characteristic dimensions of such local features. Thus, it might be expected that ground motions containing substantial high frequencies would yield more information about building stiffness. Consequently, a better identification of the structural stiffness would be possible. Fig. 12 (Table 9) shows the identification carried out using colored noise as the input ($\Delta t = 0.025$ sec.). As observed from a comparison of Figs. 4*(a)*, 10*(a)*, and 12*(a)*, the estimate using the high frequency input is much improved. It may be noted, though, that for all three cases [Figs. 4*(b)*, 10*(b)*, and 12*(b)*], the quality of history match is excellent.

Conclusions and Discussion

1 A systematic computationally efficient scheme for identifying parameters in systems that can be expressed by linear hyperbolic differential equations has been developed. The standard method of sensitivity coefficients requires the system equations to be integrated $n + 1$ times, at each iteration step, where n is the number of grid points. The integration needs to be carried out once for the current **k**. Perturbations of the n dimensioned **k** vector lead to the remaining n equations to be integrated to get all the sensitivity coefficient. The technique used here requires just two integrations at each iteration step—the integration of the system equation and its adjoint. Since the number of iterations for a typi-

Table 7 Scaled N-S component of 1940 El Centro earthquake motion data used (Case: 2)

Time Length of Record Analyzed	Normalized Mean Error in Estimate[1]	Normalized Standard Dev. of Error in Estimate[2]	Normalized R.M.S. Error in Estimate[3]	Mean Error in Displacement History Match at Roof[4]	Standard Dev. of Error in History Match at Roof[5]	Weighting Factor of Second Derivative Penalty
INITIAL GUESS						
(0 sec.)	0.0%	15.84%	19.84%	-0.07×10^{-4}	0.07×10^{-2}	
5 secs.	3.76%	11.15%	11.77%	-0.07×10^{-4}	0.37×10^{-3}	0.225×10^{-9}
15 secs.	2.05%	7.42%	7.69%	-0.14×10^{-5}	0.35×10^{-3}	0.675×10^{-9}
30 secs.	2.04%	7.42%	7.70%	0.24×10^{-5}	0.57×10^{-3}	0.135×10^{-8}

Table 8 Scaled N-S component of 1940 El Centro earthquake motion data used (Case: 3)

Time Length of Record Analyzed	Normalized Mean Error in Estimate[1]	Normalized Standard Dev. of Error in Estimate[2]	Normalized R.M.S. Error in Estimate[3]	Mean Error in Displacement History Match at Roof[4]	Standard Dev. of Error in History Match at Roof[5]	Weighting Factor of Second Derivative Penalty
INITIAL GUESS						
(0 sec.)	1.43%	19.05%	19.11%	0.105×10^{-4}	0.72×10^{-3}	-
5 sec.	0.29%	18.88%	18.88%	-0.74×10^{-7}	0.62×10^{-3}	0.27×10^{-9}
15 sec.	-1.52%	16.48%	16.55%	0.25×10^{-4}	0.88×10^{-3}	0.81×10^{-9}
30 sec.	-1.82%	16.55%	16.65%	-0.12×10^{-5}	0.40×10^{-3}	0.16×10^{-8}

Table 9 Identification using colored noise (Case: 2) $\Delta t = 0.025$ sec.

Time Length of Record Analyzed	Normalized Mean Error in Estimate[1]	Normalized Standard Dev. of Error in Estimate[2]	Normalized R.M.S. Error in Estimate[3]	Mean Error in Displacement History Match at Roof[4]	Standard Dev. of Error in History Match at Roof[5]	Weighting Factor of Second Derivative Penalty
INITIAL GUESS						
(0 sec.)	33.3%	0%	33.3%	0.64×10^{-4}	0.915×10^{-2}	
5 sec.	-2.35%	8.1%	8.44%	-0.636×10^{-4}	0.167×10^{-2}	0.69×10^{-9}
10 sec.	0.071%	4.61%	4.61%	0.234×10^{-5}	0.182×10^{-2}	0.138×10^{-8}
20 sec.	-0.11%	2.39%	2.40%	-0.36×10^{-4}	0.135×10^{-2}	0.276×10^{-8}

cal problem may be anywhere from 75 to 100, the method proposed yields an enormous computational economy, especially when n is large.

2 Instead of the inequality constraints usually employed in such problems, penalty functions in terms of the first and second derivations of the stiffness with respect to height were used. These functions were found very helpful in additionally constraining the estimates, though they could not eliminate the nonuniqueness problem completely.

3 Application of the technique to the estimation of building stiffnesses (as a function of height) through the use of basement and roof records and the proviso that the building can be modeled by a continuous shear beam indicate that

(*a*) the convergence towards the true estimates can only be reached when the initial guesses are sufficiently close to the exact values. For cases of constant stiffness distributions and linearly varying distributions, initial constant guess distributions may differ from the mean of the exact distribution by as much as 20 to 30 percent and yet converge rapidly to the correct distributions.

(*b*) the speed of convergence is greatly influenced by a proper preconditioning of the estimates before longer and longer records can be efficiently handled. A sequential updating of the estimate, gradually using longer and longer time lengths is most efficient.

(*c*) the problem of nonuniqueness of the estimate may become an important one in the sense that a numerically obtained estimate $k(x)$, obtained after a good history match is established, may differ widely from the true function $k(x)$, depending on the initial guess, $k_0(x)$, that is chosen and the true function $k(x)$. This points to the fact that responses of model and system may differ for inputs different from those used in the identification process.

(4) the success of the identification process is strongly dependent on the nature of the ground inputs

- (*a*) for ground motions, which contain a few predominant frequencies, the identification, beyond a certain record length, is only marginally improved by taking longer and longer record lengths.
- (*b*) broad band inputs containing high frequency waves whose wavelengths are comparable to the characteristic lengths of the local stiffness variations yield good stiffness estimates.

4 As of today, several investigators have used the history matching of roof records to be a criterion for establishing the correctness of the parameters of the models, usually of lumped mass kind, representing structural systems. The nonunicity of such an estimation indicated here shows that even under ideal measurement conditions, though such matching may be a necessary condition in establishing the parameter values within the framework of an assumed model, the constraints imposed may not be sufficient to tie down the estimates uniquely.

Acknowledgments

The authors are grateful for the several suggestions and comments offered to them by Dr. George Gavalas, California Institute of Technology. Thanks are due to Drs. P. C. Jennings, G. W. Housner and D. E. Hudson of Caltech and Dr. S. Masri at the U. S. C. for their critical reading of the manuscript.

References

1 Udwadia, F. E., and Trifunac, M. D., "Time and Amplitude Dependent Response of Structures," *Intl. J. Earthq. Engr. and Struct. Dyn.*, Vol. 2, 1974, pp. 359–378.

2 Hudson, D. E., "Strong-Motion Instrumental Data on the San Fernando Earthquake of Feb. 9, 1971," Earthquake Engineering Research Laboratory, California Institute of Technology, Pasadena, Sept. 1971.

3 Berg, G. V., "Finding System Properties from Experimentally Observed Modes of Vibration," Primeras Jornadas Argentinas de Ingenieria Antisismica, April 1962.

4 Nielsen, N., "Dynamic Response of Multistory Buildings," Earthquake Engineering Research Laboratory, EERL, California Institute of Technology, Pasadena (1964).

5 Ibañez, P., "Identification of Dynamic Structural Models from Experimental Data," Ph.D. Thesis, University of California, Los Angeles, 1972.

6 Jennings, P. C., "Spectrum Techniques for Tall Buildings," Proceedings of the Fourth World Conference on Earthquake Engineering, San Tiago, Chile, Vol. 2, Session A3, 1969.

7 Wood, J., "Analysis of the Earthquake Response of a Nine Story Steel Frame Building During the San Fernando Earthquake," Earthquake Engineering Research Laboratory, EERL 72-04, California Institute of Technology, Pasadena, October, 1972.

8 Jacquard, P., and Jain, C., "Premiability Distribution from Field Pressure Data," *Society of Petroleum Engineers Journal*, Vol. 5, No. 6, Dec. 1965.

9 Carter, R., Kemp, L., Pierce, A., and Williams, D., "Performance Matching with Constraints," *Society of Petroleum Engineers Journal*, Vol. 14, No. 2, April 1974.

10. Chen, W., Seinfeld, J., Gavalas, G., and Wasserman, M., "A New Algorithm for Automatic History Matching," *Society of Petroleum Engineers Journal*, Vol. 14, No. 6, Dec. 1974.

11 Chevant, Guy, "Identification of Distributed Systems," Proceedings of the Third IFAC Symposium on Identification and System Parameter Estimation, The Hague, 1973.

12 Polak, E. "An Historical Survey of Computational Methods in Optimal Control," *S.I.A.M. Review*, Vol. 15, No. 2, April 1973.

13 Udwadia, F. E., "On Some Unicity Problems in Building Systems Identification from Strong Motion Records," Proceedings of Fifth European Conference on Earthquake Engineering, 1975.

APPENDIX 1

$$\text{Mean error} = \sum_{i=1}^{N} (k_{\text{estimated}} - k_{\text{exact}})/N$$

1 Normalized mean error $= \dfrac{\sum_{i=1}^{N} (k_{\text{estimated}} - k_{\text{exact}})/N}{\sum_{i=1} k_{\text{exact}}/N}$

2 Normalized standard deviation in estimate $= \sqrt{\dfrac{\sum_{i=1}^{N} [(k_{\text{estimated}} - k_{\text{exact}}) - \text{mean error}]^2}{N[\sum_{i=1}^{N} k_{\text{exact}}/N]^2}}$

3 Normalized RMS error in estimate $= \sqrt{\dfrac{\sum_{i=1}^{N} (k_{\text{estimated}} - k_{\text{exact}})^2}{N[\sum_{i=1}^{N} k_{\text{exact}}/N]^2}}$

4 Mean error in displacement history $= \Delta = \sum_{i=1}^{p} (w_{\text{observed}} - w_{\text{calculated}})$, where $p\Delta t = T$ match at roof

5 Standard deviation of error in history $= \sqrt{\sum_{i=1}^{N} (w_{\text{observed}} - w_{\text{calculated}} - \Delta)^2/P}$ match at roof